# A Full Reference Video Quality Measure based on Motion Differences and Saliency Maps Evaluation

B. Ortiz-Jaramillo, A. Kumcu, L. Platisa and W. Philips
*UGent-iMinds-IPI, St-Pietersnieuwstraat 41, Gent, Belgium*
{*bortiz, akumcu, ljiljana.platisa, philips*}*@telin.ugent.be*

Keywords: Dense Optical Flow, Psychophysics, Saliency Maps, Temporal Distortions, Video Quality Assessment.

Abstract: While subjective assessment is recognized as the most reliable means of quantifying video quality, objective assessment has proven to be a desirable alternative. Existing video quality indices achieve reasonable prediction of human quality scores, and are able to well predict quality degradation due to spatial distortions but not so well those due to temporal distortions.
In this paper, we propose a perception-based quality index in which the novelty is the direct use of motion information to extract temporal distortions and to model the human visual attention. Temporal distortions are computed from optical flow and common vector metrics. Results of psychovisual experiments are used for modeling the human visual attention. Results show that the proposed index is competitive with current quality indices presented in the state of art. Additionally, the proposed index is much faster than other indices also including a temporal distortion measure.

## 1 INTRODUCTION

Video-based applications such as video coding, digital television, surveillance and tele-medicine, are becoming more common in everyday life. Quality control is important in those applications for increasing the quality of service, which can be degraded due to compression, network packet delay, and packet loss, among others. In this field, video quality assessment (VQA) has an important role in evaluating and improving the performance of video-based applications. VQA can be grouped into two main categories: subjective and objective methods. Subjective VQA is performed by a group of persons, who evaluate (processed or corrupted) video sequences according to certain well-defined criteria such as ITU standards (ITU-R-Recommendation-BT.500-11, 1998). The results are typically explained in terms of Differential Mean Opinion Scores (DMOS). This methodology represents the most realistic system of measuring the opinion of humans toward video or image quality (ITU-R-Recommendation-BT.500-11, 1998), (VQEG, 2003). However, such tests are complex, expensive, and time consuming. Hence, objective (automatic) assessment is a more desirable alternative.

Objective VQA uses computer algorithms for computing quality scores that should correlate well with the subjective assessment provided by human evaluators. In general, those algorithms are classified into natural visual characteristic methods (NVC) or perceptual oriented methods (POM) (Chikkerur et al., 2011). NVC methods use statistical measures (mean, variance, histograms) and/or visual features (blurring, blocking, texture, visual impairments) for computing quality scores, for example the Video Quality Model (VQM) (Pinson and Wolf, 2004), the motion compensated structural similarity index (MC-SSIM) (Moorthy and Bovik, 2010) or video quality assessment by decoupling additive impairments and detail losses (VQDM) (Li et al., 2011). VQM is computed by using local spatio-temporal statistics which are extracted and combined to obtain a quality score. MC-SSIM uses a popular still image quality metric and block-based motion compensation for computing errors along motion trajectories. VQDM separates detail losses and additive impairments by subtracting a restored version of each frame from the reference image. Then, both distortions are pooled and combined for computing a single quality score.

POM methods have been designed based on results of physiological and/or psychovisual experiments, e.g., weighted structural similarity index (wSSIM) (Wang and Li, 2007), and motion-based video integrity evaluation index (MOVIE) (Seshadrinathan and Bovik, 2010). wSSIM uses the structural similarity index for measuring local image differences, termed quality maps. For computing a unique quality score from those quality maps, a spatiotemporal weighted mean is used. Those weighting factors are computed based on a Bayesian optimal observer hypothesis. MOVIE uses a Gabor filter bank specifically designed based on physiological findings for mimicking the visual system response. The video quality evaluation is carried out from two components (spatial and temporal distortions). Spatial distortions are computed as squared differences between Gabor coefficients of the reference and processed sequences. Temporal distortions are obtained from the mean square error between reference and processed sequences along motion trajectories computed over the reference video. Although many video quality assessment algorithms have been proposed, many of them do not explicitly account for temporal artifacts which occur in video sequences. For instance, in VQM, MC-SSIM, VQDM and wSSIM, motion information is only used to design weights to pool quality maps into a single quality score for the video. However, weights based on temporal information do not necessarily account for temporal distortions (Seshadrinathan and Bovik, 2010). Despite of the direct use of motion in MOVIE, the computational complexity of the algorithm makes practical implementation difficult as it relies on 3-D optical flow and filter bank computation (Moorthy and Bovik, 2010).

Since motion is critical for measuring quality, video quality metrics have to take into account temporal (motion compensation mismatch, jitter, ghosting, and mosquito noise, ...) and spatial (blocking, blurring and edge distortion, ...) distortions (Yuen and Wu, 1998). Considering that the area of still image quality assessment has attained maturity, spatial distortions are usually well captured by current quality metrics (image quality metrics achieve correlations above 0.9 between subjective and objective scores, in most of the databases) (Seshadrinathan and Bovik, 2010). However, temporal distortions are not well estimated by existent methods (Seshadrinathan and Bovik, 2010). In addition, motion information is only used to compute weights and/or extracted from a filter bank response in current methods, which is generally, as stated previously, inaccurate for capturing temporal distortions (Wang and Li, 2007) (Seshadrinathan and Bovik, 2010) (Moorthy and Bovik, 2010). Considering that most of the existing VQA algorithms compute motion information indirectly, it is necessary to fully investigate the contribution of motion to human perception of quality. Therefore, we believe that temporal distortions or errors due to motion should be computed directly from the local motion field instead of using the methods listed above.

In this paper, we propose a POM-based quality index in which the main contribution comes from the direct use of motion information to extract temporal distortions and to model the human visual attention (HVA). On the one hand, since the human visual system (HVS) infers motion from the changing pattern of light in the retinal image (Watson and Ahumada, 1985), we compute motion errors from optical flow differences because it assumes the same changing pattern of light from one frame to the other. On the other hand, we performed psychovisual experiments for modeling directly the HVA instead of using assumptions like in (Wang and Li, 2007). We design saliency maps based on the results of the psychovisual experiments which are later used in the pooling strategy. Considering that the proposed quality index is specifically designed for measuring temporal distortions, we combine it with the well know spatial structural similarity index (SSIM) in order to account for both types of distortions. Results show that the proposed quality index is competitive with current methods presented in the state of art. Additionally, the proposed index is much faster than other indices also including a temporal distortion measure.

The rest of the paper is organized as follows. Section 2 introduces background information and Section 3 describes the proposed quality index. Results are in Section 4 and conclusions in Section 5.

## 2 BACKGROUND

### 2.1 Dense Optical Flow

Dense optical flow is one of the most popular mechanisms for estimating motion in video analysis with great accuracy in several tasks such as tracking, video quality assessment, and human speed perception, among others (Barron et al., 1992), (Wang and Li, 2007), (Daly, 1998). Optical flow, in video analysis, refers to the changes in grey values caused by the relative motion between a video camera and the content of the scene, for example motion of objects, surfaces, and edges. Mathematically, optical flow assumes that pixel intensities are translated from one frame to the next (this is called brightness constancy), i.e., $I(x,y,t-1) = I(x+u,y+v,t)$, where $I(x,y,t)$ is the intensity of the pixel located at position $(x,y)$ and time $t$. Here, $(u,v)$ is the velocity vector or optical flow which can depend on $x$ and $y$. In this field, the Lucas-Kanade algorithm is one of the most well-known and widely used optical flow estimation methods because it accounts for the most desirable features in optical flow computation (accuracy, low computational cost, and good noise tolerance) (Barron et al., 1992). Therefore, the Lucas-Kanade algorithm is used as optical flow estimator in the proposed methodology as explained in Section 3.

## 2.2 Saliency Maps

Spatial regions which attract the HVS are called salient regions. Usually, humans do not pay attention to every detail in the visual field but concentrate on some salient regions (Marat et al., 2009). By combining the salient regions of the visual field, a map of attentional field called saliency map is obtained. Particularly, saliency maps are highly related to the motion and contrast of objects (Wang and Li, 2007). Usually, salient regions for videos are computed by using spatial and temporal saliency maps. Both maps are often inspired by recent results of either physiological or psychovisual experiments (Max-Planck-institute, 2013), (Marat et al., 2009). In this work, saliency maps are computed based on local image entropies, motion and the nonlinear mapping of these features. Here, the nonlinear mapping is designed based on results of psychovisual experiments. The psychovisual experiments use alternative force choice tasks in which one or more stimuli are presented to several human subjects. In such tasks, human subjects are prompted to indicate whether or not they can see the stimulus. Thereafter, the behavior of the given psychovisual task (e.g., proportion of trials the stimulus was seen) is related to some physical characteristic of the stimulus (e.g., contrast, entropy, motion) by using a function, termed the psychometric function. In this work we design an *one alternative force choice* (1AFC) task for designing the proposed nonlinear mapping used in the saliency map computation, see Sections 3.2 and 3.4 for further details.

## 2.3 Performance of Video Quality Indices

The performance of video quality indices is evaluated by comparing the predicted quality to the human scores. The human scores, termed DMOS, are given by subjective quality assessment of a set of previously prepared video sequences. The predicted quality, termed *pDMOS*, is the output of the objective quality index after a nonlinear transformation. The nonlinear transformation is performed with the purpose of facilitating comparisons between models in a common space of analysis (VQEG, 2003). Such nonlinear transformation is defined as $pDMOS = \frac{b_0}{1+\exp(-(b_1+b_2 q))}$, where $b_0,\ldots,b_2$ are constants with the best fit to the DMOS and $q$ is the output by the objective video quality index, for instance, the output of MOVIE algorithm.

Once the nonlinear transformation is applied, the performance of the objective models is evaluated by computing various metrics between DMOS and *pDMOS*. Such metrics evaluate the following three aspects: prediction accuracy, prediction monotonicity and prediction consistency (VQEG, 2003). Prediction accuracy refers to the ability of predicting the subjective quality score with low error, this aspect is measure by using the Pearson correlation coefficient (PCC). Prediction monotonicity is the degree to which predictions of the model agree with the magnitudes of subjective quality scores, this aspect is measure with the Spearman rank-order correlation coefficient (SROCC). Prediction consistency is the degree to which the model maintains prediction accuracy over a range of different video test sequences, this can be measure by using root mean-squared error (RMSE).

# 3 PROPOSED QUALITY INDEX

It is well know that temporal distortions in video alter motion trajectories of pixels, for example motion compensation mismatch, jitter and ghosting, and/or introduce a false perception of motion such as mosquito noise (Yuen and Wu, 1998), (Seshadrinathan and Bovik, 2010). Noteworthy is that temporal distortions affecting video sequences are perceived by humans as motion. By taking advantage of the convenient relationship between motion perception and optical flow (Watson and Ahumada, 1985), one can assume that there is available a good registration of motion, i.e., there is translation of pixel intensities from one frame to the next. In such case, given two video sequences $I_r$ and $I_p$ such that $I_p$ is a processed or corrupted version of $I_r$, we say that both sequences exactly match when optical flows are equal. That is, $U_r = U_p$ and $V_r = V_p$, where $U_r$, $V_r$ and $U_p$, $V_p$ are the $x$ and $y$ components of the velocity vectors of the reference and processed video sequences, respectively. However, when temporal distortions appear in $I_p$, optical flows in both video sequences do not match and the optical flow in $I_p$ may change. Thus, a common vector metric can help to measure optical flow differences for detecting temporal distortions. Particularly, we use the root squared error ($\sqrt{(U_r - U_p)^2 + (V_r - V_p)^2}$) because it is the most common and widely used metric for comparing optical flows (Barron et al., 1992). Thus, our temporal quality index is developed by assuming optical flow equality in the absence of temporal distortions. In

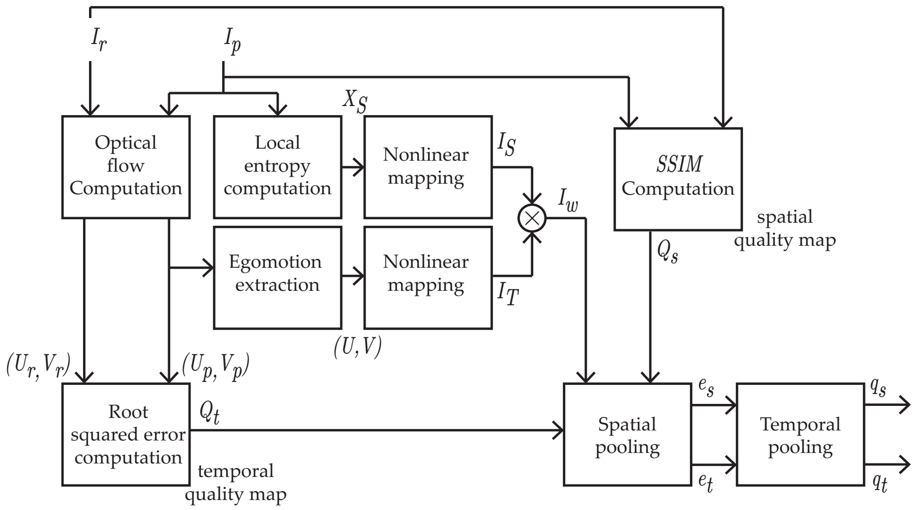


Figure 1: Flow chart of the proposed quality indices.

Figure 1 the flow chart of the proposed quality index is shown.

## 3.1 Spatial and Temporal Quality Maps

The optical flow for the reference and processed videos, noted by $(U_r,V_r)$ and $(U_p,V_p)$ and shown in Figures 2(c) and 2(d), are computed from the video sequences $I_r$ and $I_p$, shown in Figures 2(a) and 2(b). For achieving a compromise between simplicity and accuracy, optical flows are computed by using the pyramidal refined implementation of the Lucas-Kanade algorithm as discussed in (Lucas and Kanade, 1981). In this paper, optical flows are computed by using 3 scales and 3 iterations. Thereafter, temporal distortions are computed pixel by pixel using the root squared error, which results in a temporal quality map, termed $Q_t$, (see Figure 2(h)). Also, from $I_r$ and $I_p$ we compute the spatial quality map ($Q_s$) by using the SSIM as discussed in (Wang et al., 2004). An example of the spatial quality map is found in Figure 2(i).

## 3.2 Spatial-temporal Saliency Map

The saliency maps are computed frame by frame by transforming visual characteristics of the video sequences with nonlinear functions. The nonlinear functions are thoroughly explained in Section 3.4. We compute the saliency maps from the processed sequence because the artifacts may change the HVA. For computing the spatial saliency map we replace each pixel in the processed frames with the normalized entropy of its surrounding neighborhood, termed $X_S$. The normalized entropy is used assuming that it is more likely to attract the HVA into regions with high information content than to regions with low information content. Then, each normalized entropy is mapped with a psychometric function to obtaining the spatial saliency map $I_S = P_S(X_S)$, where $P_S(X_S)$ is the proportion of times that the stimulus is perceived with motion given $X_S$ (see Section 3.4). We use such nonlinear mapping because it is an indication of the probability of seen a moving object giving its entropy. An example of the spatial saliency map is shown in Figure 2(e).

The temporal saliency map is computed by mapping the magnitude of the optical flow with a nonlinear function, i.e., $I_T = P_T(Mg)$, where $Mg = 2f\tan^{-1}\left(\frac{\|(U,V)\|dx}{2d}\right)$ (see Section 3.4). Here, $dx$, $d$, $f$ and $\|(U,V)\|$ are the size in centimeters of each pixel, distance from the viewer to the display, the frame rate and the magnitude of the optical flow in the processed sequence after camera motion extraction, respectively. Camera motion is extracted with the purpose of approximating the eye fixation of the HVA (Wang and Li, 2007). The camera motion or egomotion $(U_g,V_g)$ is estimated from $(U_p,V_p)$. Here, egomotion is estimated by using a six parameters affine model and lest squares estimation as discussed in (Yao et al., 2001). The local motion field $(U,V)$ is obtained as $(U,V) = (U_r,V_r) - (U_g,V_g)$. This nonlinear mapping is performed with the purpose of approximating optical flow to the results obtained by Daly. Figure 2(f) shows an example of the temporal saliency map. The final proposed spatio-temporal saliency map is obtained by multiplying pixel by pixel both maps like in Pinson and Wolf (Pinson and Wolf,

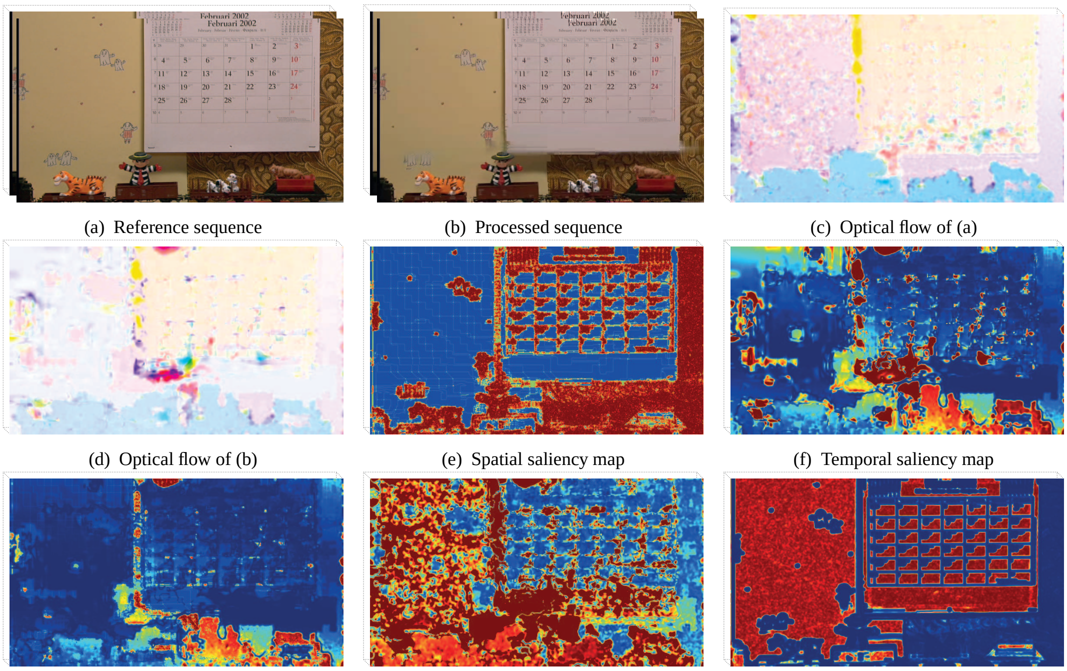

(a) Reference sequence (b) Processed sequence (c) Optical flow of (a)
(d) Optical flow of (b) (e) Spatial saliency map (f) Temporal saliency map
(g) S-T saliency map (h) Root squared error (i) SSIM

Figure 2: Illustrations of the proposed quality metric. S-T: Spatio-temporal. Optical flows of the reference and processed sequences are color coded (direction is coded by hue, length by saturation). EE, SSIM and saliency maps are color coded from blue to red.

2004), $I_w = I_S I_T$, (see Figure 2(g)).

### 3.3 Pooling Strategy

The proposed pooling strategy is based in the use of the saliency maps explained in Section 3.2, i.e., we use weighting functions for obtaining spatial and temporal quality indices. The spatio-temporal saliency map ($I_w$) is used in the pooling strategy as follows:

$$e_t(t) = \sqrt{\frac{\sum_{x,y} I_w(x,y,t) Q_t^2(x,y,t)}{\sum_{x,y} I_w(x,y,t)}} \quad (1a)$$

$$e_s(t) = \frac{\sum_{x,y} I_w(x,y,t) Q_s(x,y,t)}{\sum_{x,y} I_w(x,y,t)}, \quad (1b)$$

where, $e_s(t)$ and $e_t(t)$ are the evolution across time of spatial and temporal distortions, respectively. Finally, $e_t(t)$ and $e_s(t)$ are pooled over time to obtain a spatial and temporal quality indices describing the quality of the video sequence $I_p$. Here, the temporal pooling is performed by using a weighted mean of the temporal evolution of distortions (see Equation (2a) and (2b)).

$$q_t = \sqrt{\frac{\sum_t \bar{I}_w(t) e_t^2(t)}{\sum_t \bar{I}_w(t)}} \quad (2a)$$

$$q_s = \frac{\sum_t \bar{I}_w(t) e_s(t)}{\sum_t \bar{I}_w(t)}, \quad (2b)$$

where $\bar{I}_w(t) = \sum_{x,y} I_w(x,y,t)$. Thus, $q_t$ and $q_s$ give more importance to frames with high salient regions than frames with low salient regions, i.e., frames with objects and/or regions that are most likely to be seen. For combining the spatial and temporal indices, we use the following nonlinear mapping: $pDMOS = \frac{b_0}{1+\exp(-(b_1+b_2 q_t+b_3 q_s))}$. Here, $b_0,\ldots,b_3$ are also constants with the best fit to the DMOS.

### 3.4 Psychophysical Experiments for Nonlinear Transformations

Here, we built the nonlinear transformations by assuming that most of the objects are static or nearly to static. Objects with a significant amount of motion provide a high information content for the HVA and therefore an object fixation is obtained. Also, it is well know that the HVA pays more attention to regions with high contrast because it is more likely to see motion at high contrast regions than at low contrast regions (Hammett and Larsson, 2012). To build the function $P_S$, we ran a 1AFC with two human subjects. One subject is naive and the other possess knowledge in the field of VQA. For this, we independently presented several stimuli to each subject. The subject is prompted to indicate whether or not they can see motion in the stimulus. The stimuli are generated by tak-

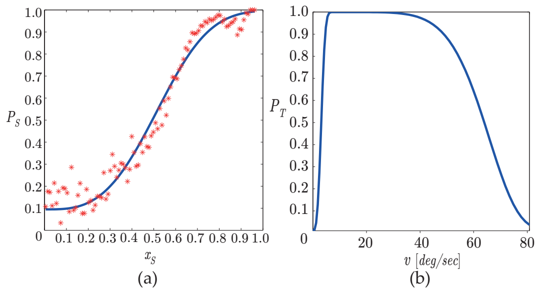


Figure 3: (a) Spatial and (b) temporal mapping functions, $P_S$ and $P_T$, respectively. Asterisks are the proportion of times the stimulus is perceived with motion for each normalized entropy $X_S$. The blue line is the best fit of the functions.

ing random blocks of $15 \times 15$ pixels per 200 millisecond from the LIVE database (Seshadrinathan et al., 2010), which is enough for a human subject to discriminate whether or not they can see motion (Watson and Ahumada, 1985). For each block, the normalized entropy is computed as $X_S = \frac{h_B}{h_U}$, where $h_B$ is the entropy of the block and $h_U \approx 7.8$ bits. The assumption is that the HVA is attracted more to regions with high information content than to regions with low information. By using the normalized entropy and the 1AFC collected data a psychometric function can be estimate. A psychometric function is typically a sigmoid function, such as the Weibull, logistic, cumulative Gaussian, or Gumbel distribution. We choose the Weibull function because is the function that most easily and accurately fits the obtained data. Thus, the psychometric function is defined as $P_S(X_S) = 1 - \exp(-(X_S/\alpha_S)^{\beta_S})$, where $\alpha = 0.58$ and $\beta = 3.16$ are constants to best fit the obtained data. Here, we set the parameters using the maximum likelihood method as discussed in (Kingdom and Prins, 2010). Figure 3(a) shows the obtained psychometric function with its respective real data.

To build the temporal saliency map, we use the results obtained by Daly (Daly, 1998). In that work the author found that the human eye cannot follow objects with velocities higher than 80 deg/sec; in such cases the saliency is null. Also, he demonstrated that the saliency reaches its maximum with motions values between 6 deg/s and 30 deg/s. We fit a nonlinear mapping function to the values obtained by Daly. We found that the following function give good results: $P_T(Mg) = (1 - \exp(-(Mg/\alpha_1)^{\beta_1}))(\exp(-(Mg/\alpha_2)^{\beta_2}))$, where $\alpha_1 = 3.5$, $\alpha_2 = 66.5$, $\beta_1 = 3.1$ and $\beta_2 = 7$. The parameters for $P_T$ function were empirically determined in order to fit the findings of Daly. Figure 3(b) shows the obtained function.

# 4 RESULTS AND DISCUSSION

In this paper two video quality databases are used: the LIVE Video Quality Database (Seshadrinathan et al., 2010) and the IVP Subjective Quality Video Database (Zhang et al., 2011). Each database contains 10 source video sequences, the Live database contains 10 standard television videos (resolution of $768 \times 432$) and the IVP contains 10 high definition videos (resolution of $1920 \times 1088$). Each of those video sequences are processed to acquire 150 and 128 test videos in the LIVE and IVP databases, respectively. Each test video is processed by using one of the following methods: wireless distortion, IP distortions, H.264 compression or MPEG-2 compression. Each database provides a DMOS value per sequence, obtained through subjective evaluations conducted by the respective authors.

Here, the proposed quality index is compared to the following popular video quality indices: i) Peak signal to noise ratio (PSNR) as a benchmark, ii) video quality model (VQM) (Pinson and Wolf, 2004), iii) weighted structural similarity index (wSSIM) (Wang and Li, 2007), iv) motion-based video integrity evaluation index (MOVIE) (Seshadrinathan and Bovik, 2010) and v) video quality assessment by decoupling detail losses and additive impairments (VQAD) (Li et al., 2011). Performances are computed as explained in Section 2.3.

Table 1 shows the performance of the considered video quality indices appraised for the LIVE and IVP video quality databases. The results show that the proposed quality index performs better than PSNR, VQM and wSSIM and is competitive with MOVIE and VQAD in both databases. For instance, the proposed quality index performs better than VQAD in the IVP database and slightly worse in the LIVE database. Compared with MOVIE the proposed quality index performs slightly worst in LIVE database, however, MOVIE is computationally intensive taking around 6-8 and 20-24 hours in video sequences of 250-frames $768 \times 432$ and $1920 \times 1088$ (which is impractical for any application), respectively. Then, results of methods that cannot be obtained within a practical time span, i.e. 1 hour or more, are not reported in Table 1. The rest of the methods are computational simpler than the proposed method. However, those methods do not include a temporal distortion measure which is crucial in video quality assessment.

The proposed quality index performs better in one database than the other. In order to understand the difference in performance, we study the residuals of the nonlinear model and the DMOS given in the LIVE database. Figure 4 shows the residuals of the pro-

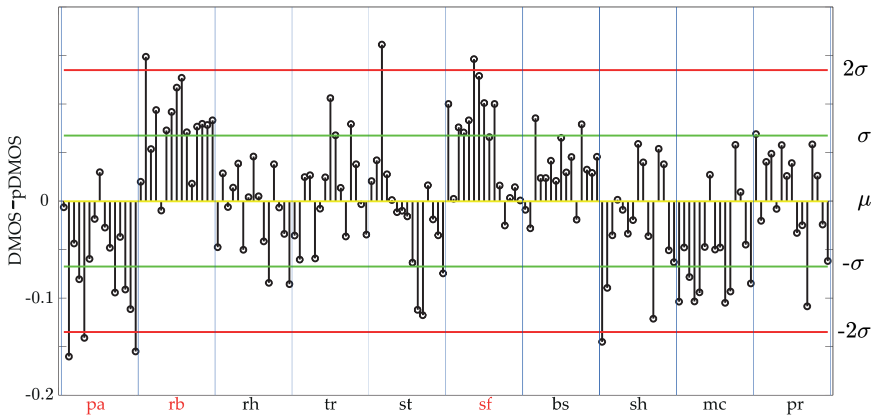


Figure 4: Residuals of the proposed quality index in LIVE database. $\mu$ and $\sigma$ are the mean and standard error, respectively. Video sequences in red means that the proposed quality index achieve the worst performance.

Table 1: Performance of considered video quality metrics appraised for the LIVE and IVP Video Quality Databases. *The computational time is computed for algorithms running in Matlab (Laptop with CPU intel core i3 2.27GHz and 4GB ram) for 250 frames of size 768 × 432. + C++ implementation.

| | LIVE | | | IVP | | | |
|---|---|---|---|---|---|---|---|
| **Method** | **RMSE** | **PCC** | **SROCC** | **RMSE** | **PCC** | **SROCC** | Time*[min] |
| PSNR | 9.109 | 0.562 | 0.539 | 0.759 | 0.687 | 0.694 | 0.15 |
| VQM | 7.932 | 0.723 | 0.702 | 0.767 | 0.672 | 0.685 | 2.5 |
| wSSIM | 8.843 | 0.596 | 0.584 | 0.803 | 0.640 | 0.640 | 37 |
| MOVIE + | 6.435 | 0.811 | 0.789 | – | – | – | 360 |
| VQAD | **6.216** | **0.824** | **0.818** | 0.659 | 0.782 | 0.787 | 1.2 |
| Proposed | 6.723 | 0.791 | 0.783 | **0.576** | **0.839** | **0.843** | 18 |

posed quality index for the LIVE database. The plot was divided in 10 horizontal sections (blue lines) representing each video in the LIVE database. The videos are named according to (Seshadrinathan et al., 2010): river bed (rb), mobile and calendar (mb), rush hour (rh), blue sky (bs), park running (pr), station (st), tractor (tr), sunflower (sf), pedestrian area (pa), shields (sh). In Figure 4, an error is significant or is considered an outlier when the error is greater than or equal to $\pm 2\sigma$, where $\sigma$ is the standard error. The worst performance was achieved on pa, rb and sf. That is, most of the residuals are close to the red line in Figure 4. This poor performance is mainly due to three reasons: large occluded regions (pa), large regions with similar texture or without texture (sf, rb). On the one hand, pa is a sequence in which a considerable number of people walk in the street. Some of those people are located or walk close to the camera, hiding the other people. Thus, when a person or object is hidden or occluded the computed motion from the Lucas-Kanade algorithm is not reliable. On the other hand, sf is a sequence in which high similar textured regions are displaced due to camera motion. Since the motion detection algorithm is based in local region searching, the optical flow can be unreliable when similar pixel values are found. The same concept applies to rb with the difference that this sequence is homogeneous. Since the proposed quality index was designed assuming a good motion registration and the three cases presents unreliable optical flow computation, the expected root squared error is also unreliable and this affect the quality index. Then, the inconsistencies in performance are mainly due to the number of occluded areas and large regions with similar texture presented in each video sequence. That means, it is necessary to include a mechanism for measuring reliability of the optical flow for improving the results presented in this paper. Despite this drawback the proposed quality index performs well compared with current methods in the stated of art. Also, the proposed index have the advantage of computing temporal distortions directly which can be used for further improvements in designing objective video quality indices.

## 5 CONCLUSIONS

We proposed a video quality index based on visual attention models and optical flow errors which successfully captures temporal distortions when a good quality optical flow registration is available. The visual attention model was built using spatial and temporal saliency maps based on psychovisual studies. The spatial saliency map is based in novel psychovisual experiments run by the authors. The temporal saliency map was built using recent findings in the area of motion analysis. Temporal errors were computed directly from optical flows by using standard vector metrics. In general, the proposed quality index is competitive with current methods presented in the state of art. Additionally, the proposed index is much faster than other indices also including a temporal distortion measure. The main drawback of the proposed quality index is that it is necessary to assume perfect motion registration which leads to inconsistencies of performance within the databases tested in this work. We prove that this behavior is mostly due to three reasons: large occluded regions, large regions with same texture and/or without texture. Despite this drawback the proposed quality index performs well and the results presented in this work could offer a good starting point for further development. Also, the proposed index have the advantage of using temporal information directly instead of using weights to pool quality maps which in general do not necessarily account for temporal distortions.

Since the proposed methodology is highly dependent on the quality of the optical flow registration, the study and incorporation of a proper mechanism for measuring optical flow reliability is proposed as future work. Also, the comparison with other methods and the evaluation of different databases remains as future work. We proposed a video quality index based on visual attention models and optical flow errors which successfully captures temporal distortions when a good quality optical flow registration is available. The visual attention model was built using spatial and temporal saliency maps based on psychovisual studies. The spatial saliency map is based in novel psychovisual experiments run by the authors. The temporal saliency map was built using recent findings in the area of motion analysis. Temporal errors were computed directly from optical flows by using standard vector metrics. In general, the proposed quality index is competitive with current methods presented in the state of art. Additionally, the proposed index is much faster than other indices also including a temporal distortion measure. The main drawback of the proposed quality index is that it is necessary to assume perfect motion registration which leads to inconsistencies of performance within the databases tested in this work. We prove that this behavior is mostly due to three reasons: large occluded regions, large regions with same texture and/or without texture. Despite this drawback the proposed quality index performs well and the results presented in this work could offer a good starting point for further development. Also, the proposed index have the advantage of using temporal information directly instead of using weights to pool quality maps which in general do not necessarily account for temporal distortions.

Since the proposed methodology is highly dependent on the quality of the optical flow registration, the study and incorporation of a proper mechanism for measuring optical flow reliability is proposed as future work. Also, the comparison with other methods and the evaluation of different databases remains as future work.

## ACKNOWLEDGEMENTS

This work was financially supported by the iMinds ICON Telesurgery project, a project co-funded by iMinds, a research institute founded by the Flemish Government. Companies and organizations involved in the project are BARCO, Unilabs Teleradiology BVBA, and CandiT-Media BVBA, with project support of IWT. Part of the work has been performed in the project PANORAMA, co-funded by grants from Belgium, Italy, France, the Netherlands, and the United Kingdom, and the ENIAC Joint Undertaking.

## REFERENCES

Barron, J., Fleet, D., Beauchemin, S., and Burkitt, T. A. (1992). Performance of optical flow techniques. In *IEEE Computer Society Conference on Computer Vision and Pattern Recognition*, pages 236–242.

Chikkerur, S., Sundaram, V., Reisslein, M., and Karam, L. (2011). Objective video quality assessment methods: A classification, review, and performance comparison. *IEEE Transactions on broadcasting*, 57(2):165–182.

Daly, S. (1998). Engineering observations from spatiovelocity and spatiotemporal visual models. In *Human Vision and Electronic Imaging III*.

Hammett, S. and Larsson, J. (2012). The effect of contrast on perceived speed and flicker. *Journal of Vision*, 12(12):1–8.

ITU-R-Recommendation-BT.500-11 (1998). Methodology for the subjective assessment of the quality of television pictures. ITU, Geneva, Switzerland.

Kingdom, F. and Prins, N. (2010). *Psychophysics A practical introduction*. Elsevier, London, 1st edition.

Li, S., Ma, L., and Ngan, K. (2011). Video quality assessment by decoupling additive impairments and detail losses. In *Third International Workshop on Quality of Multimedia Experience (QoMEX)*.

Lucas, B. and Kanade, T. (1981). An iterative image registration technique with an application to stereo vision. In *Imaging Understanding Workshop*.

Marat, S., Phuoc, T., Granjon, L., Guyader, N., Pellerin, D., and Guérin-Dugué (2009). Modelling spatio-temporal saliency to predict gaze direction for short videos. *International journal of Computer Vision*, 82(3):231–243.

Max-Planck-institute, M.-P.-i.-f.-b.-c. (2013). Brain research on non-human primates. http://hirnforschung.kyb.mpg.de/en/homepage.html.

Moorthy, A. and Bovik, A. (2010). Efficient video quality assessment along temporal trajectories. *IEEE transactions on circuits and systems for video technology*, 20(3):1653–1658.

Pinson, M. and Wolf, S. (2004). A new standardized method for objectively measuring video quality. *IEEE transactions on broadcasting*, 50(3):312–322.

Seshadrinathan, K. and Bovik, A. (2010). Motion tuned spatio-temporal quality assessment of natural videos. *IEEE transactions on image processing*, 19(11):335–350.

Seshadrinathan, K., Soundararajan, R., Bovik, A., and Cormack, L. (2010). Study of subjective and objective quality assessment of video. *IEEE transactions on image processing*, 19(6):1427–1441.

VQEG, V.-Q.-E.-G. (2003). The validation of objective models of video quality assessment, phase ii. http://www.its.bldrdoc.gov/vqeg/vqeg-home.aspx.

Wang, Z., Bovik, A., Sheikh, H., and Simoncelli, E. (2004). Image quality assessment: From error visibility to structural similarity. *IEEE transactions on image processing*, 13(4):600–612.

Wang, Z. and Li, Q. (2007). Video quality assessment using a statistical model of human visual speed perception. *Journal of optical society of America*, 24(12):B61–B69.

Watson, A. and Ahumada, A. (1985). Model of human visual-motion sensing. *Journal of optical society of America*, 2(2):322–342.

Yao, P., Evans, G., and Calway, A. (2001). Face tracking and pose estimation using affine motion parameters. In *Proceedings of the 12th Scandinavian Conference on Image Analysis*.

Yuen, M. and Wu, H. (1998). A survey of hybrid mc/dpcm/dct video coding distortions. *Signal processing*, 70:247–278.

Zhang, F., Li, S., Ma, L., Wong, Y., and Ngan, K. (2011). Ivp subjective quality video database. http://ivp.ee.cuhk.edu.hk/research/database/subjective/index.shtml.